DOI: 10.17344/acsi.2019.5025 *Acta Chim. Slov.* **2019,** *66,* 614–621

Scientific paper

The Influence of Cardboard Dust on Structural, Morphological and Mechanical Properties of Biocomposite PLA and HDPE Filaments for 3D Printing

Diana Gregor-Svetec,* Urška Stankovič Elesini, Raša Urbas, Mirjam Leskovšek and Urška Vrabič Brodnjak

University of Ljubljana, Faculty of Natural Sciences and Engineering, Department of Textiles, Graphic Arts and Design, Snežniška ulica 5, Ljubljana, Slovenia

** Corresponding author: E-mail: diana.gregor@ntf.uni-lj.si; Tel: +386 1 200 32 72*

Received: 02-05-2019

Abstract

In the material extrusion of the thermoplastic filaments, known as Fused Deposition Modelling, usually, pure thermoplastic polymers are used. Recently, the focus of the research is given to the development of new biocomposite thermoplastic materials. In our research, 3D printable biocomposite filaments, made with the addition of 50 wt.% of cardboard dust to the HDPE and PLA polymer matrix were studied. The influence of the added cardboard dust on structural, morphological and mechanical properties of the 3D printable biocomposite filaments was investigated. With the addition of the corrugated cardboard dust into the HDPE and PLA polymer matrix the changes in density, uniformity, chemical structure and transition temperatures of the samples were detected. The addition of the cardboard dust into the HDPE polymer matrix lead to low tenacity, toughness, deformability resulting in brittleness of the 3D printable biocomposite filament, whereas the addition of the cardboard dust into the PLA polymer matrix lowered tensile properties, but didn't affected bending toughness and has even improved compression strength of the 3D printable filament.

Keywords: 3D printing; filaments; PLA; HDPE; biocomposite

1. Introduction

The production of cardboard is a continuous process. Layers of paper are glued together into long, continuous strips of cardboard and are automatically cut, while the waste (small shreds) falls alongside the line. This waste needs to be removed as quickly as possible.

The corrugated cardboard industry is primarily using shredders to destroy and or to air handling their scrap material. These shredders use a rip and tear technology, to break apart the cardboard. This process is noisy and at the same time causes formation of the waste – the cardboard dust. Bigger part of unused waste cardboard is recycled and waste cardboard dust is incinerated.[1] Incineration is an expensive, rigid and technology-depended waste management strategy.[1] Burning the cardboard waste and the dust is wasteful, because incineration captures only one fifth of calories in these materials.[2]

However, another possibility is to recycle the cardboard dust by using it as a filler in polymer filaments for 3D printing. The most spread 3D printing technology is the Fused Deposition Modelling (FDM), in which thermoplastic polymer is melted into a semi-liquid state and extruded through the head onto the build platform.[3] Materials that are used in the FDM 3D printing must have suitable heat transfer characteristics and rheology i.e. behaviour of liquid flow. Thus, the most appropriate are some of the thermoplastic polymers, such as polylactic acid (PLA), acrylonitrile butadiene styrene (ABS), polyamide (PA) etc.[4]

In our research, two thermoplastic polymer filaments were used, polylactic acid (PLA) and high-density polyethylene (HDPE). The PLA is mostly amorphous. It is produced from renewable resources (i.e. corn starch or sugarcane) and is biodegradable under the suitable conditions. Since the PLA has low toughness and thermal stability, different reinforcements are used to improve its disadvantages. Regarding mentioned, the PLA matrix was, through various studies reinforced with different materi-

als, such as hemp, flax, jute, sisal and bamboo fibres, cellulose nanofibres etc.[5–11] The PLA is the most common polymer for FDM 3D printing. Properties of the PLA filament loaded with the wood particles in different levels from 0–50% were investigated by Kariza et al.[12] Results have shown that the increase of wood particles, decreased the density of the composite filaments for 3D printing. The tensile strength of the filaments increased with an addition of 10% wood, but decreased with higher wood content. At the same time, the storage modulus decreased with higher wood content, although the glass transition temperature did not change.

The composite filament from PLA, ABS, HDPE, as well as other matrices reinforced with carbon, glass or natural fibres, core-shell rubber, organic and inorganic particles, are also used in FDM application.[13]

The HDPE is highly crystalline, low density and flexible recyclable and eco-friendly material, and as shown by Kreiger et al., it has potential also in the in-home recycling of post-consumer plastic.[12] Its drawbacks are high thermal expansion, poor temperature capability, low toughness and ductility. To improve some of those drawbacks, the HDPE as matrix was reinforced with different materials such as kenaf and jute fibres, treated argan-nut shell particles, pinecone, coconut and snail shell powder, pineapple fibres etc.[14–22] Recently, the impact of addition of thermomechanical (TMP) pulp fibers (0–30% w/w) on the mechanical properties of bio-polyethylene was researched by Tarrésa et al.[23]

The HDPE filaments are also used for FDM 3D printing, though not as often as the PLA.

For the purpose of our research the PLA and the HDPE polymers were reinforced with 50 wt.% cardboard dust. The aim of our research was to determine the influence of the addition, of the cardboard dust on the structure and the properties of 3D printable filaments.

2. Materials and Methods

2. 1. Materials

Two 3D printable biocomposite filaments were produced with adding of the 50 wt.% cardboard dust into the PLA and the HDPE polymer matrix. The cardboard dust was obtained from a paper mill, as a residue in a cardboard production. The pure PLA and the HDPE 3D printable filaments were produced from commercial pellets (producer Plastika Trček, Slovenia). As a reference, 3D printable filaments made from the pure PLA and HDPE were used.

Table 1: Notation of 3D printable filaments

Sample	Polymer matrix	Added filer
PLA	PLA	/
PLA/50 c.d.	PLA	Cardboard dust (50 wt.%)
HDPE	HDPE	/
HDPE/50 c.d.	HDPE	Cardboard dust (50 wt.%)

2. 2. Testing Methods

3D printable filaments were qualitatively analysed with the FT-IR spectrometer Spectrum GX I (Perkin Elmer). Spectra were recorded over the range 4000–800 cm^{-1}, with the resolution of 4 cm^{-1}.

The density of 3D printable filaments was calculated as a ratio of mass per unit volume. The time of sound wave propagation through the 3D printable filaments in the longitudinal direction was measured using a Pulse Propagation Meter PPM-5R (H. Morgan, Co.), at a frequency of 160 Hz. The velocity of the sound waves was calculated as a ratio of the distance and the time of the pulse propagation. The thermal stability of the 3D printable filaments was measured with the Hot-stage microscopy, using the Mettler FP84HT microscopy system. Temperature measuring range was between 30–200 °C, and the rate of heating was 5 °C/min.

The analysis of the 3D printable filaments cross-section was performed by the Scanning electron microscope (SEM) JSM-6060 LV (Jeol), at different magnifications.

The dynamic Mechanical Analysis (DMA) was performed using a Q800 DMA analyser (TA Instruments). The measurements were performed in a dual cantilever bending mode on the 3D printable filaments, with the sample length of 35 mm. Measurements were performed at the frequency from 1 to 10 Hz of oscillation and temperature range 0–160 °C, with the temperature step of 3 °C/min rising to 160 °C. Depending on the temperature and the frequency, the transition temperatures, bending storage modulus (E'), bending loss modulus (E") and tan delta (tan δ) of the 3D printable polymer filaments were determined.

The mechanical properties were determined using a tensile testing machine Instron 5567 (Instron). The tensile properties of the 3D printable filaments were determined according to the ASTM D2256. The bending resistance was determined with the 2-point bending test and the compression load was measured by compressing the filament to half its thickness.

3. Results and Discussion

3. 1. Structural Characteristics

For composite materials, changes in chemical composition or interactions between the 3D printable filaments can be observed as changes in the peak intensities.[24,25]

Figure 1 shows spectra of the analysed pure PLA and the biocomposite PLA/cardboard dust 3D printable filaments in the range of wavenumber from 4000 to 800 cm^{-1}. More detailed insight into spectra can be seen in the range

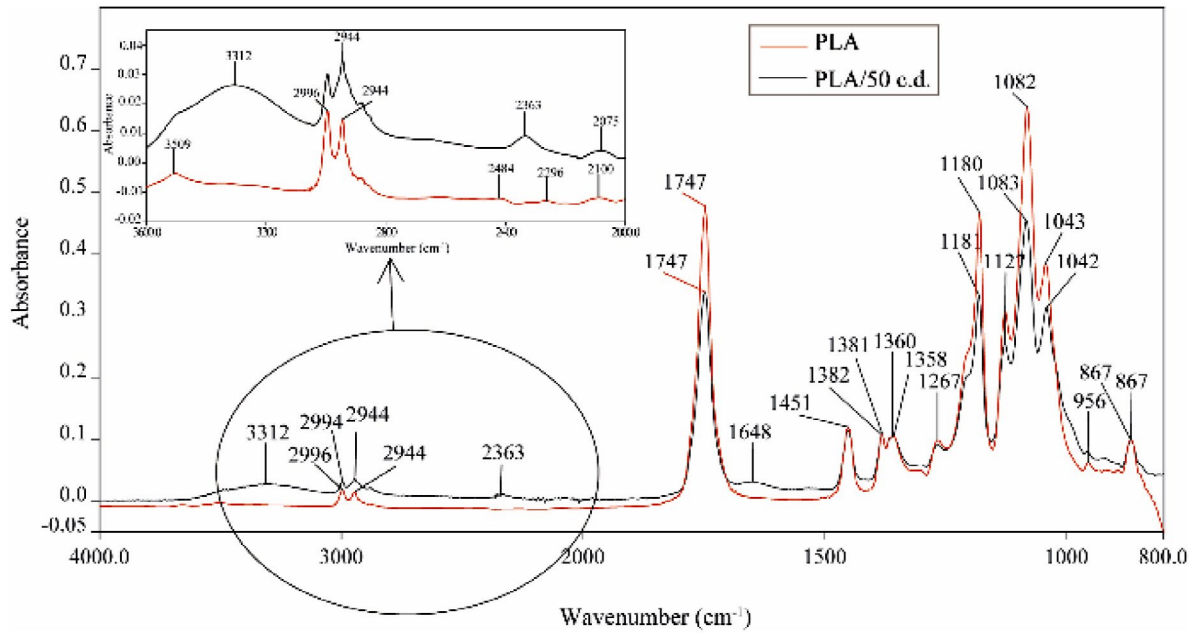

Figure 1: ATR FTIR spectra of pure PLA (PLA) and 50 wt.% PLA/ cardboard dust (PLA/50 c.d.) 3D printable filaments

of 3600 and 2000 cm^{-1}, where the differences due to the addition of the 50 wt. % cardboard dust can be observed. The peaks at 2996 and 2944 cm^{-1} are typical for the PLA, and present the stretching of the hydroxyl groups and the symmetrical and the asymmetrical stretching of the C-H groups.[26] In the sample PLA/50 c.d., the peak at 3312 cm^{-1} can be detected.[27] This confirms the presence of the cellulose in the sample, because it shows the vibration of the -OH group.[28] At pure PLA 3D printable filament, the peak at 3509 cm^{-1} can be assigned to the asymmetrical stretching of the C-H group in the PLA. This peak was also detected for the biocomposite PLA/cardboard dust 3D printable filament, but with lower intensity. In the range between 1800 and 800 cm^{-1}, PLA spectra had higher absorbance, compared to the biocomposite filament sample. In this range no significant peaks were detected, only the peak at 1648 cm^{-1}, which presents the vibrations of the CH_2 group and the vibrations of the hydrogen bonds in the cellulose. This again confirms the presence of the cellulose, though, despite the addition of the 50 wt.% corrugat-

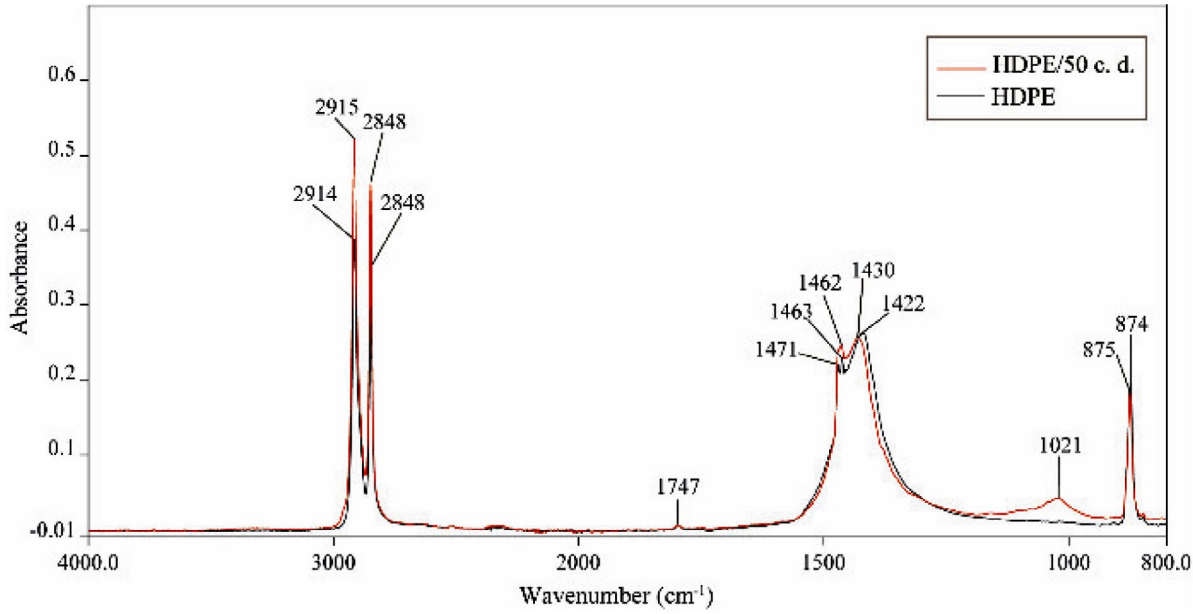

Figure 2: ATR FTIR spectra of pure HDPE (HDPE) and 50 wt.% HDPE/cardboard dust (HDPE/50 c.d.) 3D printable filaments

ed cardboard dust, the content of the PLA component stands out.

Figure 2 shows spectra of the analysed pure HDPE and the 50 wt.% HDPE/cardboard dust 3D printable filaments in the range of wavenumber from 4000 to 800 cm^{-1}. It unites the absorption bands of the polyethylene matrix and the characteristic absorption bands of the cellulose (cardboard dust). Characteristic peaks for the HDPE are in the range of 2915 and 2848 cm^{-1}, and can be assigned to the symmetrical and the asymmetrical vibrations of the CH_2 groups in the HDPE. The same is with the peaks at 875 and 874 cm^{-1}, which present the bending of the CH_2. The assigned peak at 1720 cm^{-1} corresponds to the carbonyl groups, which is the main result of the polyethylene. The peak at 1021 cm^{-1} confirmed the addition of the cellulose in the sample.[27,28] This peak corresponds to the asymmetrical vibrations of the glycosidic rings of the cellulose. From the presented spectra it can be seen that the major peaks are from the HDPE component, meaning that the filament`s surface is composed mainly from the HDPE polymer.

Table 2: Density, sound wave velocity and melting temperature of 3D printable filaments

Sample	Density (g/cm^3)	Sound wave velocity (km/s)	Melting temperature (°C)
PLA	1.260	1.77	172
PLA/50 c.d.	0.961	2.45	150
HDPE	0.995	2.05	132
HDPE/50 c.d.	0.501	1.31	150

Results presented in table 2 show that after the cardboard dust was added into the PLA polymer matrix the density of the 3D printable filament decreased for 25%, while the longitudinal speed of the sound waves traveling through the filament increased almost for 40%. The later applies that the structure of the biocomposite PLA/cardboard dust 3D printable filament (PLA/50 c.d.) is more oriented in direction of the filament axes, compared to the pure PLA 3D printable filament. The density of the 50 wt.% biocomposite HDPE/cardboard dust 3D printable filament (HDPE/50 c.d.) reduced to half its value, compared to the pure HDPE 3D printable filament. In this sample also, the sound wave velocity decreased substantially, implying that the structure is more porous with lower uniformity.

Thermal analysis has shown, that the first changes in the structure of the pure PLA 3D printable filament occurred at 147 °C, while the melting was completed at 172 °C. In the 50 wt.% biocomposite PLA/cardboard dust 3D printable filament the first changes were noticed at 120 °C. The cardboard dust part of the biocomposite firstly turned yellow, and later melted at 140 °C, whereas the PLA component completely melted at 150 °C.

On the other hand, the addition of the cardboard dust increased thermal stability of the 50 wt.% biocomposite HDPE/cardboard dust 3D printable filament for about 15%. The first change was noticed at 132 °C, where the HDPE matrix starts to melt, and the cellulose starts yellowing.

Cross-section images of the pure PLA 3D printable filament revealed relatively uniform structure without any seen additives or pores in the structure. On the other hand, the cardboard dust in the biocomposite filament (Figure 3) acts as a filler in the PLA polymer matrix, thus leaving the structure a bit more porous, less uniform and with visible particles of the cardboard dust, due to which the surface of the filament was rougher and more brittle. The pure HDPE 3D printable filament has some holes in the structure, resulting from the filament production process. The addition of 50 w.t.% of cardboard dust has profound effect on the structure of polymer matrix. With the addition the structure becomes highly porous, with visible small particles of cardboard dust in the matrix. SEM analysis has revealed better inclusion of the cardboard dust particles to the PLA matrix as to the HDPE matrix. The cross section of PLA/cardboard dust 3D printable filament (PLA/50 c.d.) shows numerous voids, caused by cardboard particles, whereas cross section of the sample HDPE/50 c.d. shows much more disrupted structure with lot of cavities present.

3. 2. Mechanical Characteristics

Mechanical properties of analysed 3D printable filaments under tensile, bending and compression load are shown in Table 3. The addition of the cardboard dust into the PLA matrix influenced the mechanical properties differently. Both PLA filaments, pure and biocomposite, are tough, thus bending filament till 15° didn't reveal noticeable difference in the bending load. The biocomposite PLA/cardboard dust 3D printable filament is weaker at loads acting in direction of filament axes, as the tensile strength was 5-times, strain at break 3-times and elastic modulus for almost 50% lower compared to the pure PLA 3D printable filament, which is in agreement with the morphological study of the filament cross-section. SEM image analysis has revealed more porous structure for the biocomposite PLA/cardboard dust 3D printable filament, compared to the pure PLA 3D printable filament, which is also confirmed with its lower density. The tensile force acting on the filament is not transported from the matrix to the filler effectively, which leads to lower strength and modulus, and also lowers the plasticity of the biocomposite. This suggests that the carboard dust, as a filler, is not bonded enough to the polymer matrix. On the other hand, the addition of the cardboard dust improves the compression toughness of the filament. By compressing the filament to half its thickness, a higher load was determined for the PLA/50 c.d. filament, because of the stiffness of the cardboard dust particles, which are imbedded in the more or

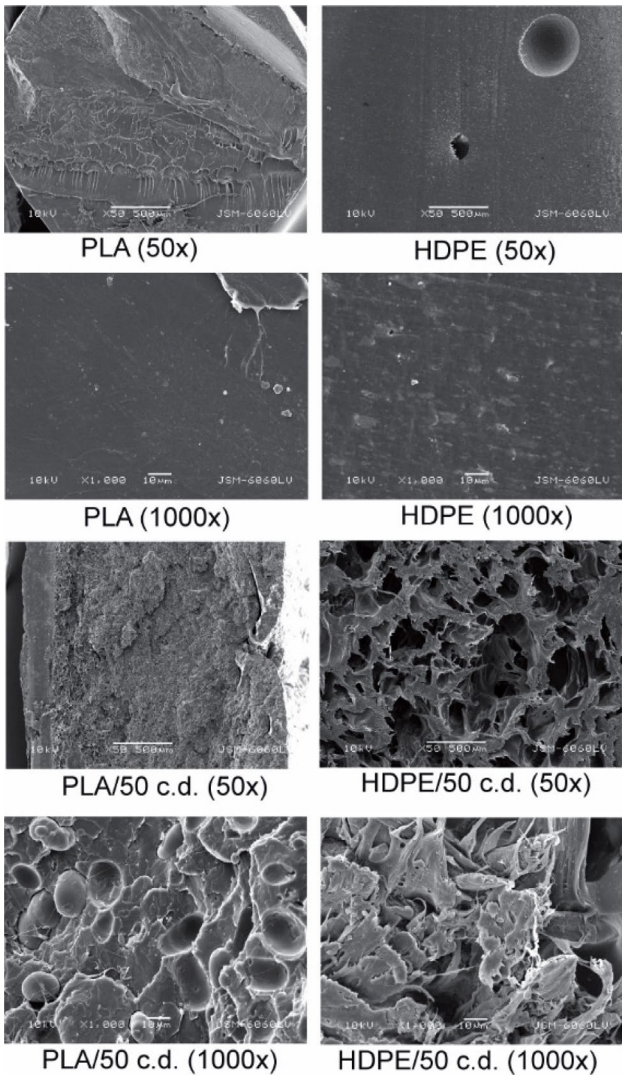

Figure 3: Cross-sections of 3D printable filaments (SEM; 50× and 1000× magnification)

less amorphous polymer matrix. A bit higher sound wave velocity propagation in the biocomposite PLA/cardboard dust 3D printable filament also suggest, that mainly amorphous structure of the polymer matrix is more oriented in the longitudinal direction of the filament, because of the filler.

The HDPE 3D printable filament is weaker compared to the PLA 3D printable filament. It has lower strength and is much more extensible. The HDPE behaves differently than the PLA under the influence of tensile load. It reaches the maximum load (198 N) at lower strain (9.94%) compared to the PLA, but then deforms under the same load (155 N) without breakage until the strain of 191% is reached. For the PLA, and both biocomposite 3D printable filaments the break occurs at maximum load. A high deterioration of the mechanical properties was determined for the biocomposite HDPE/cardboard dust 3D printable filament. This is due to the low miscibility of the HDPE polymer with the cardboard dust, thus resulting in highly porous, non-homogenous structure. The biocomposite HDPE/cardboard dust 3D printable filament is ductile, with low tensile strength, which is 8-times lower, compared to the pure HDPE 3D printable filament. It has lower toughness and resistance to bending and compression.

The reason for the higher deterioration of the mechanical properties for the biocomposite HDPE/cardboard dust 3D printable filament compared to the PLA/cardboard dust 3D printable filament is in the much weaker interfacial bonding between the filler and the matrix, and much more porous structure. The presence of the cavities confirms that the interfacial bonding between the filler and the matrix polymer is poor and weak (Figure 3). It also appears that the cardboard dust is not well distributed in the polymer matrix, especially in the sample HDPE/50 c.d. where the polymer matrix is no longer continuously distributed, and localised bundles of the cardboard dust are present, leading to poor bonding between them and to the polymer matrix. These causes stress concentration and without efficient transporting the stress between the polymer matrix and the filler, resulting in a substantially lower strength of the HDPE/cardboard dust 3D printable filament. Compounding and surface modification of the polymer matrix could improve the interfacial bonding between the filler and the polymer matrix leading to better response to stress and less deterioration of the mechanical properties.

3. 3. Dynamic Mechanical Characteristics

The dynamic mechanical properties of the samples as a function of a temperature are shown in Figures 4 to 6, while the glass relaxation transition temperatures are shown in Table 4.

Table 3: Mechanical properties of 3D printable filaments

	Tensile strength (MPa)	Strain at break (%)	Elastic modulus (GPa)	Load at bending (N)	Load at compression (kN)
PLA	56.46	12.46	1.45	2.71	8.85
PLA/50 c.d.	11.57	4.12	0.84	2.73	10.19
HDPE	16.76	191 (9.94*)	0.39	1.97	5.75
HDPE/50 c.d.	2.05	7.60	0.12	0.71	1.50

* strain at maximum force

As can be seen from Figure 4, the biocomposite HDPE and PLA filaments respond differently to dual cantilever bending in the temperature relaxation interval due to the very different structural characteristics. The curve slope of the bending storage modulus E' of the pure HDPE sample slowly decreases through the wider temperature interval (from 0 to 140 °C) and thus implies on semi-crystalline viscoelastic polymer structure. During heating, the bending storage modulus decreases due to the movement of the macromolecules in the amorphous region (5). In the case of the pure PLA sample, the rapid drop of the storage modulus E' curve through very narrow temperature interval (from 50 to 60 °C) characterises the amorphous nature of the polymer. The movement of the molecular segments, which leads to their equilibrium conformations and increase in free volume, are achieved in very narrow relaxation interval. The storage modulus E' of the HDPE filament is much higher as in the case of the PLA through the whole temperature scale, suggesting that the HDPE filament has more ordered structure with greater interactions among the molecular chains compared to the PLA filament structure. The PLA filament is thus more prone to deformation (more flexible), while the HDPE filament is stiffer with higher elasticity.

After the cardboard dust is mixed into the HDPE polymer (HDPE/50 c.d.), the bending storage modulus E' drastically decreases for 91.1% and stay low through the whole temperature range. The noticed decrease of the storage modulus is more intensive for the pure HDPE filament compared to the biocomposite HDPE/50 c.d. sample. The pure HDPE sample dissipated more energy influenced by the macromolecules movement, which resulted in the higher plastic deformation of the HDPE filament (Figure 5), with decreased elasticity and increased flexibility.

In contrary, the biocomposite PLA/50 c.d. shows very similar elastic response as the pure PLA (as can be seen from the Figure 4), which suggests that the cardboard dust does not have any significant influence on the connection between the PLA molecular chains, only that the drop of the elasticity, influenced by the heating, occurred earlier. The elasticity of both the PLA and the PLA/50 c.d. filament is still low, indicating lower stiffness than the pure HDPE filament, but higher than the biocomposite filament HDPE/50 c.d.

Table 4: Glass transition temperature of the 3D printing filament

Sample	Relaxation transition temperature* T_g [°C]
PLA	59.39
PLA/50 c.d.	58.04
HDPE	55.89
HDPE/50 c.d	42.71

* Tg was determined from the curves of the bending storage modulus.

The relaxation transition temperatures (Tg) of the pure PLA and HDPE filaments are higher as for their biocomposite PLA/50 c.d. and HDPE/50 c.d. filaments. The temperature of relaxation transition decreases just slightly in the case of the PLA filaments (from 59.4 °C for the pure PLA to 58.0 °C for the PLA/50 c.d.), while apparent decrease was detected in the case of the HDPE filaments (from 55.9 °C for the pure HDPE to 42.7 °C for the HDPE/50 c.d.). By adding the cardboard dust, the free volume between the adjacent molecular chains increases, which contributes to easier and earlier slippage of the structure segments, required less energy to gain the relaxation state.

The curves of bending loss modulus E" (Figure 5) for the HDPE and the PLA filaments are different in shape according to the mentioned semicrystalline and amorphous structure of both filaments, respectively. The curve of loss modulus E" of the pure HDPE filaments is wider, which suggests that movement of the macromolecules took more time and caused the dissipate energy to take place at wider

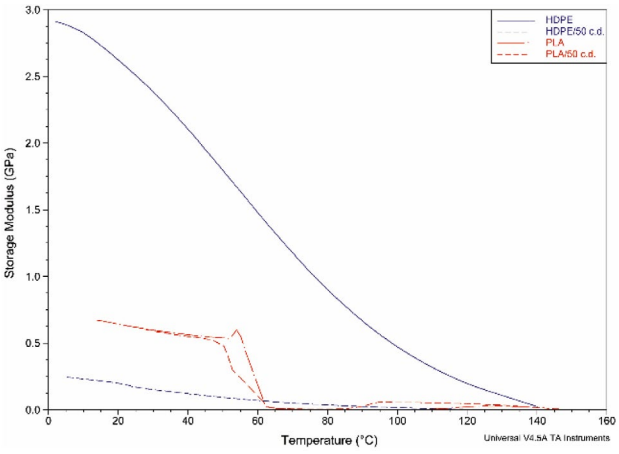

Figure 4: Bending storage modulus of 3D printing filaments at 10 Hz of oscillation

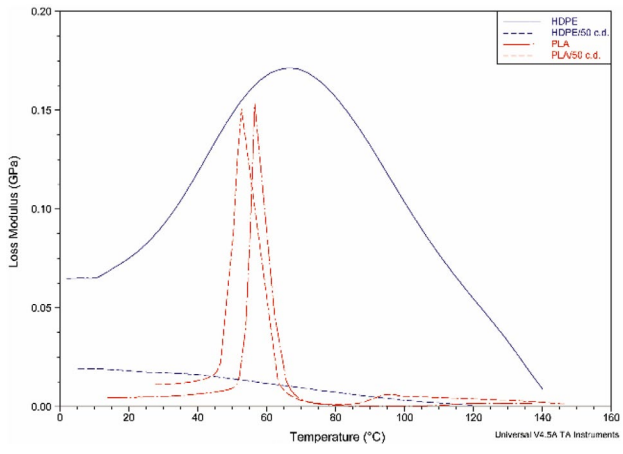

Figure 5: Bending loss modulus of 3D printing filaments at 10 Hz of oscillation

temperature interval. With elevated temperature, the curve of the loss modulus increased and reached the peak at 65 °C. After that, the loss modulus starts to decrease. After the cardboard dust is mixed with the HDPE, the value of the loss modulus decreased drastically, with no noticeable peak in modulus. According to the values of the loss modulus, the biocomposite filament HDPE/50 c.d. is less prone to the plastic deformations as the pure and more rigid HDPE filament. The peaks of the loss modulus E" for both PLA filaments are more prominent and were reached at 56.6 °C and 52.7 °C for the pure PLA and the biocomposite filament PLA/50 c.d., respectively. Both curves are narrow in the interval of relaxation transition because of the dominant amorphous regions.

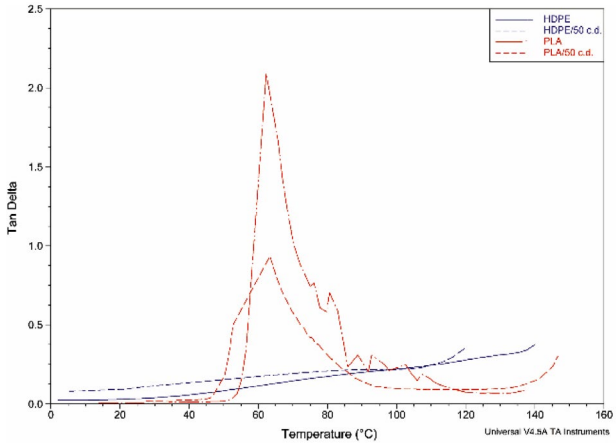

Figure 6: Loss factor (tan δ) of 3D printing filaments at 10 Hz of oscillation

The damping properties of the filaments are shown in Figure 6. From the diagram can be seen that the value of the loss factor (tan δ) was significantly higher in the case of the pure PLA filament, compared to the PLA/50 c.d. and the HDPE filaments. Since the pure PLA has loss factor (tan δ) above 1, the filament shows more viscous than elastic properties, while the pure HDPE with loss factor far below 1 is more elastic, due to its higher crystallinity. In the pure PLA filament, the movement of the molecular segments is more intensive as in the PLA/50 c.d. in which incorporated cardboard dust reduced the intensity of macromolecules movement. The PLA/50 c.d. filament exhibits lower damping properties and with loss factor (tan δ) around 1 that implies approx. equal share of the plastic and the elastic component in the structure. Comparing to the HDPE/50 c.d. filament, the pure HDPE has lower tan δ values, influenced by the greater elastic response of the structure, as seen in Figure 4.

4. Conclusions

The structural, the morphological and the mechanical properties of two biocomposite 3D printable filaments (the 50 wt.% HDPE/cardboard dust and the 50 wt.% PLA/cardboard dust) were compared with the properties of the pure HDPE and the PLA 3D printable filaments. Behaviour of the 3D printable filaments under tensile, bending and compression load was evaluated.

The morphology of filaments is mainly nonhomogeneous and porous. SEM image analyses evidenced a heterogeneous distribution of the cardboard dust and the pores in the polymer matrix. It was established that the biocomposite 3D printable filaments have lower density, thermal stability and inferior mechanical properties in comparison to the pure filaments. With the FTIR analysis the changes in morphology, due to the addition of the cardboard dust has been confirmed. The addition of the 50 wt.% cardboard dust into the HDPE polymer matrix leads to low tenacity, toughness, deformability resulting in brittleness of the biocomposite filament, whereas the addition into the PLA polymer matrix didn't affect bending toughness and has even improved the compression strength of the 3D printable filament. When viscoelastic properties are discussed, the pure HDPE shows higher stiffness with greater elastic response than the pure PLA. With the addition of the 50 wt.% carbon dust the stiffness of the HDPE filament is significantly lowered, while it does not have any significant influence on the stiffness of the PLA/cardboard biocomposite. It follows, that PLA and HDPE 3D printed objects, both pure and composite, will be stiff when handling at ambient temperature. With increased temperature above 30 °C, the structure of the HDPE sample and therefore 3D objects will become more flexible (when used). Above this region, it is of big of importance that the 3D objects are not exposed to greater mechanical deformation, which can result in irreversible plastic deformation of the material. In the case of the PLA samples, this region is found to be above 45 °C.

Considering that most of the mechanical properties deteriorate with the addition of the 50 wt.% cardboard dust into the HDPE, it is recommended to use smaller fraction of the carbon dust, which is also cited in the references as in the research of Kariza et.al.[12]

Their research confirmed the 50% of wood content decreased the tensile properties of composite filament with PLA. When smaller amount of wood parts (10%) were used, tensile properties and storage modulus increased.

Therefore the goal of the future researches is also to find the optimal (critical) portion of the carboard dust, which does not have the significant influence on the mechanical behaviour of the material, especially the HDPE (or might even improve it).

Acknowledgement

Research is a part of the project Cel.Cycle, Discarded potentials of biomass. Programme »Potential of biomass for development of advanced materials and bio-based products« is co-financed by EU Structural Funds in Slovenia.

5. References

1. C. K. Thomas, D. Fullerton, Garbage: Recycling, and Illicit Burning or Dumping. In *The Economics of Residential Solid Waste Management,* Routledge, London, Great Britain, **2017**, pp. 81–94. **DOI:**10.4324/9781315240091-5
2. A. M. Omer, *Renew. Sust. Energ. Rev*. **2008**, *12*(9), 2265–2300.
3. D. Muck, I. Križanovskij. *3D printing*. Ljubljana, Pasadena, **2015**. **DOI:**10.1016/j.rser.2007.05.001
4. H. N. Chia, B. M. Wu, *J. Biol. Eng.* **2015**, *9*(1), 4. **DOI:**10.1186/s13036-015-0001-4
5. M. A. Sawpan, K. L. Pickering, A. Fernyhough, *Compos. Part A-Appl. S.* **2011**, *42*(3), 310–319.
6. B. Bax, J. Müssig, *Compos Sci. Technol*. **2008**, *68*, 1601–1607. **DOI:**10.1016/j.compscitech.2008.01.004
7. S. H. Lee, T. Ohkita, K. Kitagawa, *Holzforschung*. **2004**, *58*(5), 529–536.
8. C. Miao, W. Y. Hamad, *Cellulose*. **2013**, *20*(5), 2221–2262. **DOI:**10.1007/s10570-013-0007-3
9. M. Jonoobi, J. Harun, A. P. Mathew, K. Oksman, *Compos. Sci. Technol*. **2010**, *70*(12), 1742–1747. **DOI:**10.1016/j.compscitech.2010.07.005
10. T. Mokhena, J. Sefadi, E. Sadiku, M. John, M. Mochane, A. Mtibe, *Polymers* **2018**, *10*(12), 1363. **DOI:**10.3390/polym10121363
11. R. Gunti, A. V. Ratna Prasad, A. V. S. S. K. S. Gupta, *Polym Composite*. **2018**, *39*(4), 1125–1136. **DOI:**10.1002/pc.24041
12. M. Kariza, M. Serneka, M. Obućinab, M. Kitek Kuzman, *Materials Today Communications* **2018**, 14, 135–140. **DOI:**10.1016/j.mtcomm.2017.12.016
13. P. U. Chris-Okafor, C. C. Okonkwo, M. S. Ohaeke, *Am J Polym Sci*, **2018**, *8*(1), 17–21.
14. M. A. Kreiger, M. L. Mulder, A. G. Glover, J. M. Pearce, *J. Clean. Prod.* **2014**, *70*, 90–96. **DOI:**10.1016/j.jclepro.2014.02.009
15. F. M. Salleh, A. Hassan, R. Yahya, A. D. Azzahari, *Compos. Part B-Eng*. **2014**, *58*, 259–266. **DOI:**10.1016/j.compositesb.2013.10.068
16. S. Mohanty, S. K. Verma, S. K. Nayak, *Compos. Sci. Technol*. **2006**, *66*(3–4), 538–547. **DOI:**10.1016/j.compscitech.2005.06.014
17. H. Essabir, M. El Achaby, R. Bouhfid, A. Qaiss, *J. Bionic. Eng*. **2015**, *12*, 129–141. **DOI:**10.1016/S1672-6529(14)60107-4
18. J. George, S. S. Bhagawan, S. Thomas, *J. Therm. Anal. Calorim*. **1996**, *47*(4), 1121–1140. **DOI:**10.1007/BF01979452
19. S. Agayev, O. Ozdemir, *Mater Res Express*. **2019**, *6*(4), 1–10. **DOI:**10.1088/2053-1591/aafc42
20. I. O. Eze1, I. O. Igwe1, O. Ogbobe1, E. E. Anyanwu, I. Nwachukwu, International Journal of Engineering and Technologies **2016**, *9*, 13. **DOI:**10.18052/www.scipress.com/IJET.9.13
21. A. T. Vasu, C. Reddy, S. Danaboyina, G. K. Manchala, M. Chavali*, J Polym Sci Appl.* **2017**, *1:2.*
22. N. A. Patel, J. R. Shah, S. J. Thanki, *International Journal of Creative Research Thoughts (IJCRT)*. **2018,** *6*, 1244–1254.
23. Q. Tarrésa, J. K. Melbøb, M. Delgado-Aguilara, F. X. Espinachc, P. Mutjéa, G. Chinga-Carrasco, *Composites Part B.* **2018**, *153*, 70–77. **DOI:**10.1016/j.compositesb.2018.07.009
24. I. H. Kim, S. C. Lee, Y. G. Jeong, *Fiber. Polym*. **2009**, *10*(5), 687–693. **DOI:**10.1007/s12221-010-0687-6
25. S. Inkinen, M. Hakkarainen, A. C. Albertsson, A. Södergård, *Biomacromolecules*. **2011**, *12*(3), 523–532. **DOI:**10.1021/bm101302t
26. D. Edith, J. L. Six, *Appl. Surf. Sci.* **2006**, *253*, 2758–2764. **DOI:**10.1016/j.apsusc.2006.05.047
27. S. Tsuchikawa, M. Schwanninger, *Appl. Spectrosc. Rev*. **2013**, *48*(7), 560–587. **DOI:**10.1080/05704928.2011.621079
28. J. R. Riba, T. Canals, R. Cantero, *Applied spectroscopy*. **2015**, *69*(4), 442–450. **DOI:**10.1366/14-07611

Povzetek

Pri ekstrudiranju termoplastičnih filamentov, se po postopku modeliranja s spajanjem slojev, običajno uporabljajo čisti termoplastični polimeri. V zadnjem času so raziskave osredotočene na razvoj novih, biokompozitnih termoplastičnih materialov. V raziskavi smo proučili biokompozitne filamente za 3D tisk, izdelane z dodatkom 50 % kartonskega prahu v HDPE in PLA polimerno matrico. Preučevali smo vpliv dodanega kartonskega prahu na strukturne, morfološke in mehanske lastnosti biokompozitnih filamentov, namenjenih za 3D tisk. Z dodajanjem kartonskega prahu v polimerno matrico HDPE in PLA, smo zaznali spremembe gostote, enakomernosti, kemijske strukture in temperaturnih prehodov vzorcev. Dodajanje le-tega v polimerno matrico HDPE, je povzročilo znižanje trdnosti, žilavosti in deformabilnosti, kar je povzročilo krhkost biokompozitnega filamenta. Kljub temu, da je dodatek kartonskega prahu v PLA znižal natezne lastnosti, pa ni vplival na upogibno togost filamentov in vzorci imajo celo izboljšano kompresijsko trdnost.